

This work has been submitted to the IEEE for possible publication.
Copyright may be transferred without notice, after which this version may no longer be accessible.

Modeling and Analysis of Coexistence Between MLO NSTR-based Wi-Fi 7 and Legacy Wi-Fi

Suhwan Jung, Seokwoo Choi, Youngkeun Yoon, Ho-kyung Son, Hyoil Kim, *Senior Member, IEEE* *†‡§

Abstract—Wi-Fi 7 introduces Multi-link operation (MLO) to enhance throughput and latency performance compared to legacy Wi-Fi standards. MLO enables simultaneous transmission and reception through multiple links, departing from conventional single-link operations (SLO). To fully exploit MLO's potential, it is essential to investigate Wi-Fi 7's coexistence performance with legacy Wi-Fi devices. Existing approaches, however, have overlooked some crucial aspects of MLO, necessitating the development of a standards-compliant analytical framework to model the actual channel access mechanism of MLO. Therefore, this paper tries to fill the gap by proposing a set of novel Markov chains (MC) to accurately model the MLO operation aligned with multi-link backoff behaviors specified by the standard. Specifically, we design two separate MCs for AP and non-AP multi-link devices (MLD) respectively, based on which transmit and collision probabilities are derived under the saturated traffic condition. Then, we also derive closed-form expressions for the throughput of various device types in the coexistence scenario between Wi-Fi 7 and legacy Wi-Fi, including AP MLD, non-AP MLD, and legacy devices. To validate the accuracy of our proposed models, we developed an ns-3 based simulator by implementing both STR(simultaneous transmission and reception) and NSTR(non-STR) based MLO operations. Our ns-3 based extensive simulations have demonstrated that the proposed analytic model provides accurate estimates on the per-device throughput performance, while also revealing the dynamics of inter-WLAN coexistence scenarios.

Index Terms—WLAN, coexistence, Multi-Link Operation, NSTR, Markov chain

I. INTRODUCTION

Wi-Fi 7, equivalently IEEE 802.11be, introduces new features to achieve better performance than legacy Wi-Fi standards [1] and flexibility in utilizing unlicensed bands as agile as its competitors like NR-U [2]. Among them, one notable feature is Multi-Link Operation (MLO) which aims to achieve

higher data rates and lower latency by introducing a new type of devices called Multi-Link Device (MLD) that can transmit and receive data simultaneously through multiple links [3], [4], unlike legacy Single-Link Devices (SLD) performing Single-Link Operation (SLO). An MLD consists of multiple stations (STAs), each with a separate lower MAC but managed by the common upper MAC. These affiliated STAs individually exchange data through their respective channels, allowing simultaneous transmission and reception (STR) [5], [6].

STR based MLO, however, may not be possible for every MLD. While AP MLDs are considered capable of STR, non-AP MLDs may face challenges to perform STR due to IDC (In-Device Coexistence) interference caused by the proximity of transceivers on the same platform, i.e., transmission on one link self-interferes with reception on another link [7]. Hence, non-AP MLDs adopt non-STR (NSTR) instead, which only allows simultaneous transmission or simultaneous reception on multiple links to resolve IDC interference [8]. To support NSTR, the standard mandates alignment of start-times and/or end-times for the transmissions across multiple links [9].

With the advent of MLO, it is essential to accurately predict the performance of MLDs when coexisting with legacy Wi-Fi devices (i.e., SLDs). Several studies have addressed this issue using simulation-based approaches [10]–[13]. [10] utilized an ns-3 based simulator to evaluate the throughput performance of each device type in a coexistence scenario involving an AP MLD operating in STR, a non-AP MLD operating in NSTR, and legacy Wi-Fi devices. [11] also employed ns-3 simulations to investigate the impact of various EDCA-based channel access mechanisms on the throughput and latency performance in a similar coexistence scenario. [12] used ns-3 as well, to measure the performance degradation caused by IDC interference when non-AP MLDs operate in STR, comparing it with their performance operating in NSTR. In addition, [13] evaluated the coexistence performance via simulations by focusing on how latency varies with traffic load.

Simulation-based approaches, however, cannot outweigh an analytical framework due to the lack of generality and intuitions they can provide. Each simulation result is only tied to its specific topology and parameter setup, and sweeping through a meaningful range of scenarios could take hours or even days. By contrast, a model-based analytical framework

*S. Jung, S. Choi and H. Kim are with Dept. of Electrical Engineering, Ulsan National Institute of Science and Technology (UNIST), Ulsan 44919, Republic of Korea (e-mail: {fydnrltlzl, csw2055, hkim}@unist.ac.kr).

†Y. Yoon and H.-K. Son are with the Radio Research Division, Electronics and Telecommunications Research Institute (ETRI), Daejeon 34129, Republic of Korea (email: {ykyoon, hgson}@etri.re.kr).

‡Hyoil Kim is the corresponding author.

§This work was supported by Institute of Information & communications Technology Planning & Evaluation (IITP) grant funded by the Korea government (MSIT) [RS-2023-00217885, Development of integrated interference analysis technology for improving frequency utilization efficiency].

yields closed-form relations that instantly reveal how design knobs affect key performance metrics and provide insights that black-box simulation alone cannot offer. Unfortunately, only few have attempted to capture the behavior of MLDs using analytical models [14], [15]. [14] proposed a channel access scheme for NSTR in both uplink (UL) and downlink (DL) scenarios and derived the coexistence throughput performance in a closed form, but its model forcibly consolidated all affiliated STAs in an MLD into a single combined Markov chain and thus misrepresents the standard-compliant alignment and backoff dynamics. In the meantime, [15] developed an analytical model for NSTR operation in the presence of legacy devices with saturated traffic to estimate the throughput of NSTR MLDs. However, it did not account for start-time alignment, a key operation in MLO.

To fill the gaps, we propose the first standards-compliant analytical framework that conforms with the per-STA backoff procedure and mandatory alignments, jointly models AP MLD and non-AP MLDs along with legacy SLDs, and accommodates asymmetric link configurations. Specifically, this paper aims at constructing a set of novel Markov chains (MC) to reflect the correct MLO NSTR operations and to accurately derive per-device throughput for three types of coexisting devices – AP MLD, non-AP MLDs, and SLDs. Our proposed MCs should play as a key building block for future MLO mechanisms to develop more intelligent and efficient MLO-based dynamic channel access ensuring the throughput and latency fairness among various types of coexisting WLAN devices. Note that this paper’s preliminary conference version appeared at [16] which only presented AP MLD’s MC without providing a complete analysis (e.g., no derivation of stationary probabilities) nor simulation-based evaluations. On the contrary, this journal manuscript provides a full set of MCs for both AP MLD and non-AP MLD with a series of complete analysis and evaluations, thus significantly extending the scope of its preliminary version.

The paper is organized as follows. Section II overviews start-time and end-time alignments, and discusses what aspects of them have been overlooked in the literature. Section III introduces our proposed MC for an AP MLD, and derives its stationary and transmit probabilities. Similarly, Section IV proposes our novel MC for Non-AP MLDs along with the same set of derivations. Next, Section V introduces the derivation of other key parameters used in the proposed analytical framework. Then, Section VI presents ns-3 based simulations compared to the proposed analysis, showing the efficacy of our proposal along with some key lessons on the coexistence dynamics. Finally, the paper concludes with Section VII.

II. SYSTEM MODEL

We consider a WLAN coexistence scenario shown in Fig. 1, which includes an AP MLD, N_{MLD} non-AP MLDs, and N_{SLD} 802.11ax devices, where each MLD consists of two STAs to access two links. We assume a saturation traffic condition as in [17]. The AP MLD can perform STR, whereas non-AP MLDs need to operate based on NSTR.

In accordance with the standard, DL and UL transmissions should selectively apply end-time alignment and start-time

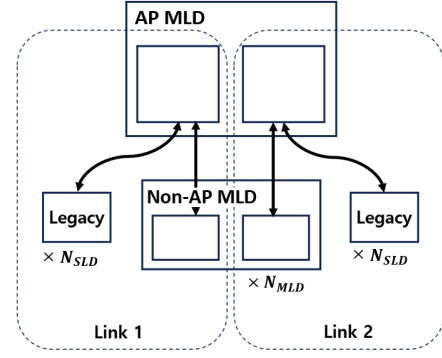


Fig. 1. Coexistence scenario between MLDs and legacy devices

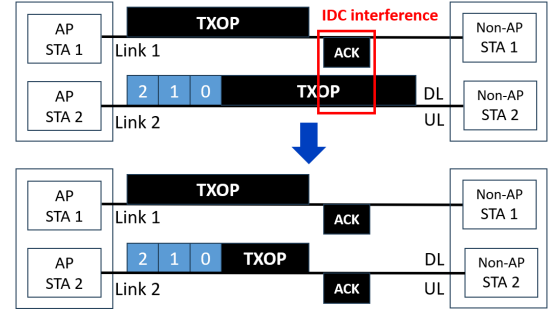


Fig. 2. Resolving IDC interference through end-time alignment

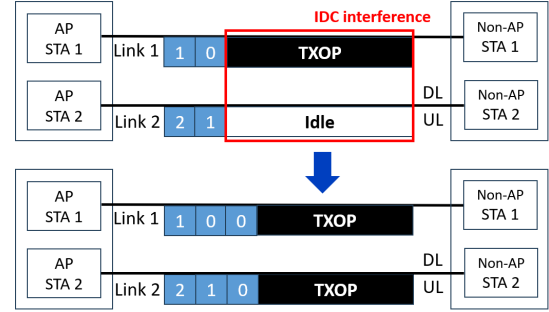


Fig. 3. Resolving IDC interference through start-time alignment

alignment as follows. First, when the AP MLD performs DL transmission, it must conduct *end-time alignment* as shown in Fig. 2. This is because DL transmission on one link incurs an ACK frame transmitted by the receiving non-AP MLD, thus inducing IDC interference on another link unless the end-times of the two transmissions are aligned. Next, when a non-AP MLD performs UL transmission, both end-time alignment and *start-time alignment* must be conducted where the latter is shown in Fig. 3, because UL transmission on one link interferes with the clear channel assessment (CCA) on another link due to IDC interference. That is, even though the other link is actually idle, it is incorrectly perceived as busy. Start-time alignment resolves this problem by synchronizing the initiation of UL transmissions across multiple links, while end-time alignment should be adopted together to prevent ACKs from the AP MLD from causing IDC interference.

Building on such standard-compliant behaviors, we consider following AP-MLD channel access rules to avoid IDC interference. When the backoff counter of one link (say Link 1, without loss of generality) in the AP MLD reaches 0, its action depends on the state of the other link (say Link 2, without loss

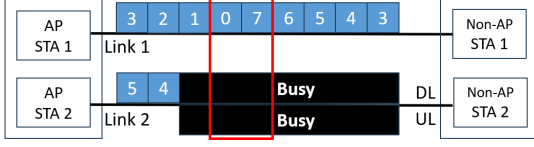


Fig. 4. Standard-compliant backoff operation during DL transmission

of generality) belonging to the same MLD, as follows:

- If Link 2 senses its channel idle, Link 1 transmits immediately.
- If Link 2 senses its channel busy without transmitting itself, Link 1 restarts its backoff procedure.
- If Link 2 is already transmitting a DL frame to a destination different from Link 1's, Link 1 transmits immediately.
- If Link 2 is already transmitting a DL frame to the same destination as Link 1's, Link 1 performs end-time alignment.

Non-AP MLDs follow a procedure different from that of the AP MLD. When Link 1's backoff counter reaches zero, it freezes until Link 2's backoff counter in the same non-AP MLD also reaches zero. If either channel becomes busy during the wait, Link 1 immediately restarts its backoff process. Once both counters reach zero, the non-AP MLD triggers a simultaneous uplink transmission on both links, applying start-time alignment as well as end-time alignment. Note that the aforementioned channel access rules reflect a most conservative interpretation of the standard, to ensure that they are fully standard-compliant.

[14] proposed backoff schemes and the corresponding MCs for AP and non-AP MLDs, taking into account the aforementioned factors. However, its MCs have the following limitations. First, they failed to accurately represent the backoff behavior of the standard-compliant MLDs. Second, each STA within an MLD independently accesses its own channel, and thus each STA's behavior should be individually modeled by a separate MC. However, [14] over-simplified it into a single 'combined' MC.

In Sections III and IV, we will first elaborate legitimate backoff behaviors of MLDs that have been overlooked by [14], and then propose our novel MCs that not only capture these behaviors but also model each link's channel access independently. To this end, we also present a detailed analysis on our MCs, including the new states and transitions required to accurately model standard-compliant MLO behaviors. Based on the proposed architectures, we will also formulate per-device per-link throughput in a closed form, inspired by the methods proposed in [17] and [18]. In particular, Section III will propose our MC for AP MLDs, while Section IV will focus on our MC for non-AP MLDs.

III. PROPOSED MARKOV CHAIN FOR AP MLD

We first explain the discrepancy between the backoff scheme in the Wi-Fi 7 standard and the one modeled in [14]. According to the standard, in case the AP MLD's backoff counter reaches 0 in Link 1 but Link 2 is busy at the moment not because of the AP's transmission, the AP MLD should restart the backoff in Link 1 while retaining the current backoff stage, as depicted in Fig. 4. The model in [14], however, failed to capture this behavior, which would incur significant analytical

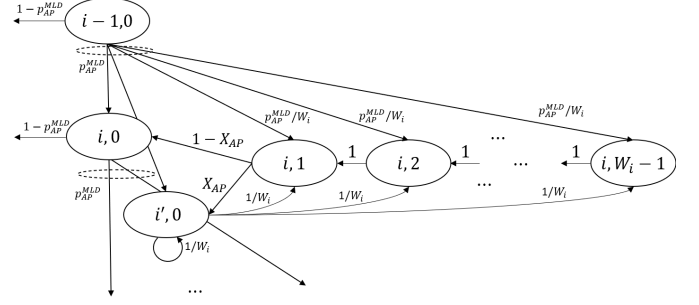


Fig. 5. Separation of state $(i, 0)$ into $(i, 0)$ and $(i', 0)$

errors especially at high traffic load where channels become busy quite frequently.

To address this issue in our MC, we introduce a state transition that restarts the backoff when the backoff counter reaches 0 in the aforementioned scenario. Unlike in the original Bianchi MC where transmission is mandatory upon reaching a backoff counter of 0, with our newly added transition, there is now an option to restart the backoff instead of forcing transmission if the other channel is busy. Fig. 5 illustrates this clearly, where the MC's state (i, k) represents the backoff stage i and the backoff counter k , with $0 \leq i \leq m$ and $0 \leq k \leq W_i - 1$. Specifically, there exist two transitions from state $(i, 1)$ into either state $(i, 0)$ or state $(i', 0)$, each corresponding to actual transmission and restarted backoff, respectively. In the figure, X represents the probability that the other link is busy not due to the AP's transmission.

Next, we build MCs for individual STAs belonging to the AP MLD. [14] assumed that the backoff of STAs within an MLD occurs simultaneously, based on which it oversimplified each STA's individual MC into a single combined MC. We rectify this by introducing a separate MC per STA, ensuring that each STA within the AP MLD independently performs backoff based on its own link state, while incorporating our new state transition proposed.

Finally, we propose a novel framework to describe the correct behavior of the AP MLD. The channel access of the AP MLD is categorized into two cases based on the destination of the packet that the AP MLD tries to transmit, as follows.

- Case 1: If the packet's destination is a legacy device (with probability $1 - \gamma$), it is transmitted via a single link following the traditional single link operation (SLO).
- Case 2: If the packet's destination is a non-AP MLD (with probability γ), MLO is performed by following the AP MLD's MC we propose.

Building upon the aforementioned enhancements, our novel MC for the AP MLD is constructed as depicted in Fig. 6.

Utilizing our proposed MC and the methodologies introduced in [17] and [18], we formulate per-device per-link throughput in a closed form. Initially, we determine the transmit probability τ that a STA transmits in a randomly chosen slot, according to: the proposed MC for the AP MLD, the MC in [14] for non-AP MLDs,¹ and the MC in [17] for legacy STAs. We denote τ of each device type by τ_{AP}^{SLD} , τ_{MLD}^I ,

¹Note that we plan to apply the proposed ideas in this paper to the MC of non-AP MLDs, as our future work.

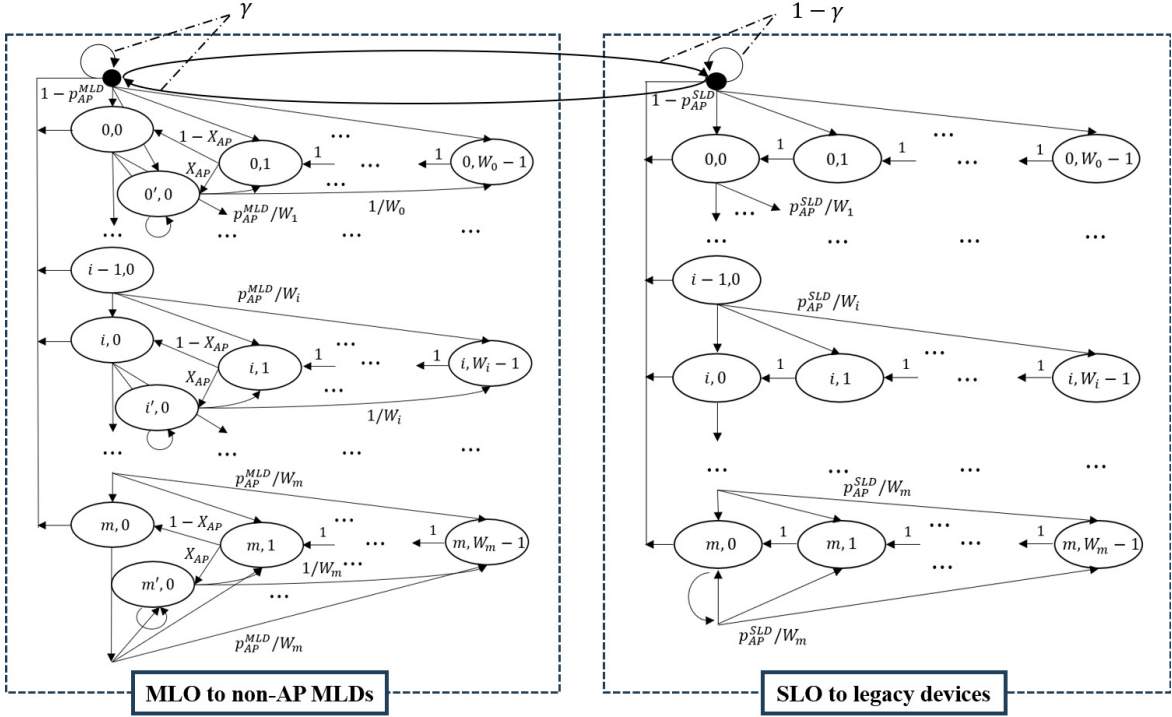


Fig. 6. The proposed MC for the AP MLD (left-hand side: DL to non-AP MLDs, right-hand side: DL to legacy devices)

τ_{SLO}^I for Case 1, and by $\tau_{\text{AP}}^{\text{MLD}}$, τ_{MLD}^{II} , τ_{SLO}^{II} for Case 2. From τ , we can derive the collision probability p that a device would experience a collision in a randomly chosen slot, where p for each device type is denoted by $p_{\text{AP}}^{\text{SLO}}$, p_{MLD}^I , p_{SLO}^I for Case 1, and by $p_{\text{AP}}^{\text{MLD}}$, p_{MLD}^{II} , p_{SLO}^{II} for Case 2.

In the sequel, we present the derivation of $\tau_{\text{AP}}^{\text{SLO}}$ and $\tau_{\text{AP}}^{\text{MLD}}$. In the meantime, the derivation of τ_{MLD}^I and τ_{MLD}^{II} will be presented in Section IV. On the other hand, the derivation of τ_{SLO}^I and τ_{SLO}^{II} closely follows the one in [17], which will be presented in Section V-A. After deriving all sorts of τ 's, various types of p 's will be derived in Section V-B.

A. Derivation of stationary probabilities

We first derive the stationary probabilities of the AP MLD's MC in Fig. 6, which consists of the MLO part (on the left) and the SLO part (on the right). The stationary probabilities are denoted by $b_{i,k}^{\text{MLD}}$ if corresponding to the MLO part, or by $b_{i,k}^{\text{SLO}}$ if corresponding to the SLO part. After deriving $b_{i,k}^{\text{MLD}}$ and $b_{i,k}^{\text{SLO}}$, we will present how to derive the two transmit probabilities $\tau_{\text{AP}}^{\text{SLO}}$ and $\tau_{\text{AP}}^{\text{MLD}}$.

First, the vertical state transitions in the MLO part among its leftmost states $(i, 0)$, $0 \leq i \leq m$ provide

$$b_{i-1,0}^{\text{MLD}} \cdot p_{\text{AP}}^{\text{MLD}} = b_{i,0}^{\text{MLD}}, \quad 0 < i < m$$

$$\Rightarrow b_{i,0}^{\text{MLD}} = (p_{\text{AP}}^{\text{MLD}})^i \cdot b_{0,0}^{\text{MLD}}, \quad 0 \leq i < m, \quad (1)$$

$$b_{m-1,0}^{\text{MLD}} \cdot p_{\text{AP}}^{\text{MLD}} = (1 - p_{\text{AP}}^{\text{MLD}}) \cdot b_{m,0}^{\text{MLD}}$$

$$\Rightarrow b_{m,0}^{\text{MLD}} = \frac{p_{\text{AP}}^{\text{MLD}}}{1 - p_{\text{AP}}^{\text{MLD}}} \cdot b_{m-1,0}^{\text{MLD}} = \frac{(p_{\text{AP}}^{\text{MLD}})^m}{1 - p_{\text{AP}}^{\text{MLD}}} \cdot b_{0,0}^{\text{MLD}}. \quad (2)$$

By Eqs. (1) and (2), we obtain

$$\sum_{i=0}^m b_{i,0}^{\text{MLD}} = \left[\frac{1 - (p_{\text{AP}}^{\text{MLD}})^m}{1 - p_{\text{AP}}^{\text{MLD}}} + \frac{(p_{\text{AP}}^{\text{MLD}})^m}{1 - p_{\text{AP}}^{\text{MLD}}} \right] b_{0,0}^{\text{MLD}} = \frac{b_{0,0}^{\text{MLD}}}{1 - p_{\text{AP}}^{\text{MLD}}}. \quad (3)$$

Similarly, the vertical state transitions in the SLO part among its leftmost states $(i, 0)$, $0 \leq i \leq m$ lead to

$$\sum_{i=0}^m b_{i,0}^{\text{SLO}} = \frac{b_{0,0}^{\text{SLO}}}{1 - p_{\text{AP}}^{\text{SLO}}}. \quad (4)$$

Next, let us consider the states with $1 \leq k \leq W_0 - 1$. For the MLO part, when $i = 0$ and $1 \leq k \leq W_0 - 1$, we obtain

$$b_{0,k}^{\text{MLD}} = \frac{W_0 - k}{W_0} [\gamma(b_{0,0}^{\text{MLD}} + b_{0,0}^{\text{SLO}}) + b_{0',0}^{\text{MLD}}], \quad 1 \leq k \leq W_0 - 1, \quad (5)$$

by applying generalized global balance equations (g.g.b.e.) to each $b_{0,k}^{\text{MLD}}$.

Building on the standard-compliant behavior described in Section II, once one link's backoff counter in an AP MLD reaches zero, its next action depends on the ongoing transmission on or the channel state of the other link. To quantify such influence between links as part of the MC, let us define X_{AP} as 'the probability that from the viewpoint of a certain link belonging to the AP MLD, the other link is busy due to the transmission either from non-AP MLD or legacy STA'. Note that X_{AP} will be derived in Section V-D since it requires

derivation of τ 's and p 's. Then, by considering the state transitions from/to state $(0', 0)$ of the MLO part, we have

$$b_{0',0}^{\text{MLD}} = X_{\text{AP}} \cdot \frac{1}{W_0} \cdot \gamma \cdot (b_{0,0}^{\text{MLD}} + b_{0,0}^{\text{SLD}}) + X_{\text{AP}} \cdot b_{0,1}^{\text{MLD}} + \frac{1}{W_0} \cdot b_{0',0}^{\text{MLD}}, \quad (6)$$

Applying Eq. (5) to the above gives

$$b_{0',0}^{\text{MLD}} = \frac{X_{\text{AP}}}{1 - X_{\text{AP}}} \cdot \frac{W_0}{W_0 - 1} \cdot \gamma \cdot (b_{0,0}^{\text{MLD}} + b_{0,0}^{\text{SLD}}). \quad (7)$$

By the state transitions from/to state $(0, 0)$ of the MLO part,

$$b_{0,0}^{\text{MLD}} = \frac{1 - X_{\text{AP}}}{W_0} \cdot \gamma \cdot (b_{0,0}^{\text{MLD}} + b_{0,0}^{\text{SLD}}) + (1 - X_{\text{AP}}) \cdot b_{0,1}^{\text{MLD}} = \gamma \cdot (b_{0,0}^{\text{MLD}} + b_{0,0}^{\text{SLD}}), \quad (8)$$

where we have applied Eqs. (5) and (7). As a result, we obtain

$$(1 - \gamma) \cdot b_{0,0}^{\text{MLD}} = \gamma \cdot b_{0,0}^{\text{SLD}}. \quad (9)$$

By Eqs. (7) and (9),

$$b_{0',0}^{\text{MLD}} = \frac{X_{\text{AP}}}{1 - X_{\text{AP}}} \cdot \frac{W_0}{W_0 - 1} \cdot b_{0,0}^{\text{MLD}}. \quad (10)$$

By combining Eqs. (5), (9), and (10), we obtain

$$b_{0,k}^{\text{MLD}} = \frac{W_0 - k}{W_0} \left[1 + \frac{X_{\text{AP}}}{1 - X_{\text{AP}}} \cdot \frac{W_0}{W_0 - 1} \right] b_{0,0}^{\text{MLD}}, \quad 1 \leq k \leq W_0 - 1, \quad (11)$$

For the SLO part, when $i = 0$ and $1 \leq k \leq W_0 - 1$, by Eqs. (3) and (4) and following the similar procedure shown earlier for the MLO part, we obtain

$$b_{0,k}^{\text{SLD}} = \frac{W_0 - k}{W_0} (1 - \gamma) (b_{0,0}^{\text{SLD}} + b_{0,0}^{\text{MLD}}), \quad 1 \leq k \leq W_0 - 1. \quad (12)$$

Then, applying Eq. (9) to Eq. (12) leads to

$$b_{0,k}^{\text{SLD}} = \frac{W_0 - k}{W_0} \cdot b_{0,0}^{\text{SLD}}, \quad 1 \leq k \leq W_0 - 1. \quad (13)$$

Next, we try to derive $b_{i,k}^{\text{MLD}}$'s for $1 \leq i \leq m$. First, the state transitions from/to each state with $i = m$ gives

$$b_{m,k}^{\text{MLD}} = \frac{W_m - k}{W_m} \cdot \left[\frac{(p_{\text{AP}}^{\text{MLD}})^m}{1 - p_{\text{AP}}^{\text{MLD}}} \cdot b_{0,0}^{\text{MLD}} + b_{m',0}^{\text{MLD}} \right], \quad 1 \leq k \leq W_m - 1. \quad (14)$$

In addition, $b_{m',0}$ can be derived as

$$1 \cdot b_{m',0}^{\text{MLD}} = \left(\frac{p_{\text{AP}}^{\text{MLD}}}{W_m} \cdot b_{m-1,0}^{\text{MLD}} + \frac{p_{\text{AP}}^{\text{MLD}}}{W_m} \cdot b_{m,0}^{\text{MLD}} + b_{m,1}^{\text{MLD}} \right) \cdot X_{\text{AP}} + \frac{1}{W_m} \cdot b_{m',0}^{\text{MLD}}. \quad (15)$$

Applying Eqs. (1), (2), and (14) to the above provides

$$b_{m',0}^{\text{MLD}} = \frac{W_m}{W_m - 1} \cdot \frac{X_{\text{AP}}}{1 - X_{\text{AP}}} \cdot \frac{(p_{\text{AP}}^{\text{MLD}})^m}{1 - p_{\text{AP}}^{\text{MLD}}} \cdot b_{0,0}^{\text{MLD}}. \quad (16)$$

Then, by combining Eqs. (14) and (16), we conclude that

$$b_{m,k}^{\text{MLD}} = \frac{W_m - k}{W_m} \left[1 + \frac{X_{\text{AP}}}{1 - X_{\text{AP}}} \cdot \frac{W_m}{W_m - 1} \right] \frac{(p_{\text{AP}}^{\text{MLD}})^m}{1 - p_{\text{AP}}^{\text{MLD}}} b_{0,0}^{\text{MLD}}, \quad 0 \leq k \leq W_m - 1. \quad (17)$$

Second, following the procedure above similarly, the state transitions at each state for $1 \leq i \leq m - 1$ provide

$$b_{i,k}^{\text{MLD}} = \frac{W_i - k}{W_i} [p_{\text{AP}}^{\text{MLD}} \cdot b_{i-1,0}^{\text{MLD}} + b_{i',0}^{\text{MLD}}], \quad 0 \leq k \leq W_i - 1. \quad (18)$$

By combining the above with Eq. (1), we get

$$b_{i,k}^{\text{MLD}} = \frac{W_i - k}{W_i} [(p_{\text{AP}}^{\text{MLD}})^i \cdot b_{0,0}^{\text{MLD}} + b_{i',0}^{\text{MLD}}], \quad 0 \leq k \leq W_i - 1. \quad (19)$$

Moreover, the state transitions regarding $b_{i',0}^{\text{MLD}}$ lead to

$$1 \cdot b_{i',0}^{\text{MLD}} = X_{\text{AP}} \cdot \frac{p_{\text{AP}}^{\text{MLD}}}{W_i} \cdot b_{i-1,0}^{\text{MLD}} + X_{\text{AP}} \cdot b_{i,1}^{\text{MLD}} + \frac{1}{W_i} \cdot b_{i',0}^{\text{MLD}}. \quad (20)$$

By applying (1) and (19) to the above, we obtain

$$b_{i',0}^{\text{MLD}} = \frac{W_i}{W_i - 1} \cdot \frac{X_{\text{AP}}}{1 - X_{\text{AP}}} \cdot (p_{\text{AP}}^{\text{MLD}})^i \cdot b_{0,0}^{\text{MLD}}. \quad (21)$$

Finally, applying Eq. (21) to Eq. (19) gives us

$$b_{i,k}^{\text{MLD}} = \frac{W_i - k}{W_i} \cdot \left[1 + \frac{X_{\text{AP}}}{1 - X_{\text{AP}}} \cdot \frac{W_i}{W_i - 1} \right] \cdot (p_{\text{AP}}^{\text{MLD}})^i \cdot b_{0,0}^{\text{MLD}}, \quad 1 \leq k \leq W_i - 1. \quad (22)$$

In the SLO part, for $1 \leq i \leq m$, the corresponding MC closely follows the MC structure in [17], from which we can obtain

$$b_{i,k}^{\text{SLD}} = \frac{W_i - k}{W_i} \cdot b_{i,0}^{\text{SLD}}, \quad 1 \leq i \leq m, \quad 0 \leq k \leq W_i - 1. \quad (23)$$

where

$$b_{i,0}^{\text{SLD}} = (p_{\text{AP}}^{\text{SLD}})^i \cdot b_{0,0}^{\text{SLD}}, \quad 1 \leq i \leq m - 1, \\ b_{m,0}^{\text{SLD}} = \frac{(p_{\text{AP}}^{\text{SLD}})^m}{1 - p_{\text{AP}}^{\text{SLD}}} \cdot b_{0,0}^{\text{SLD}}, \quad i = m. \quad (24)$$

Since the sum of stationary probabilities should be 1, we get

$$1 = \sum_{i=0}^m \sum_{k=0}^{W_i-1} b_{i,k}^{\text{MLD}} + \sum_{i'=0'}^{m'} b_{i',0}^{\text{MLD}} + \sum_{i=0}^m \sum_{k=0}^{W_i-1} b_{i,k}^{\text{SLD}} \\ = \sum_{k=0}^{W_0-1} b_{0,k}^{\text{MLD}} + \sum_{k=0}^{W_m-1} b_{m,k}^{\text{MLD}} + \sum_{i=1}^{m-1} \sum_{k=0}^{W_i-1} b_{i,k}^{\text{MLD}} + \sum_{i'=0'}^{m'} b_{i',0}^{\text{MLD}} \\ + \sum_{k=0}^{W_0-1} b_{0,k}^{\text{SLD}} + \sum_{k=0}^{W_m-1} b_{m,k}^{\text{SLD}} + \sum_{i=1}^{m-1} \sum_{k=0}^{W_i-1} b_{i,k}^{\text{SLD}}. \quad (25)$$

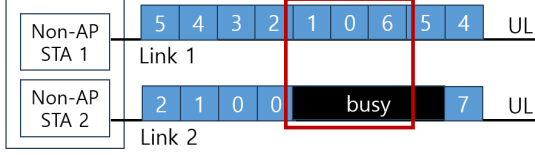


Fig. 7. Standard-compliant backoff operation during UL transmission

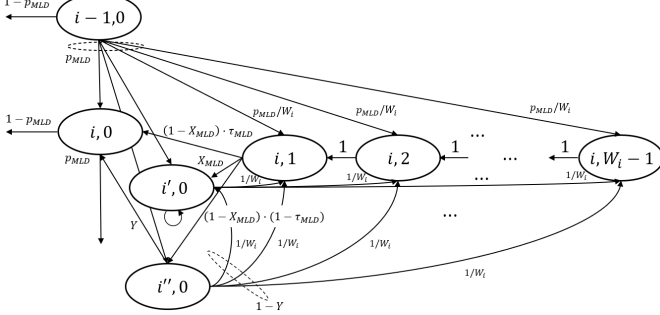


Fig. 8. Separation of state $(i, 0)$ into $(i, 0)$, $(i', 0)$ and $(i'', 0)$

By applying Eqs. (10) through (24) to the above, we obtain

$$1 = \lambda_1 \cdot b_{0,0}^{\text{MLD}} + \lambda_2 \cdot b_{0,0}^{\text{SLD}}, \quad (26)$$

$$\lambda_1 := \left[\frac{1}{1 - p_{\text{AP}}^{\text{MLD}}} + \sum_{i=0}^{m-1} \left(\frac{W_i - 1}{2} + \frac{X_{\text{AP}}}{1 - X_{\text{AP}}} \frac{W_i}{2} \right) (p_{\text{AP}}^{\text{MLD}})^i \right. \\ \left. + \frac{W_m - 1}{2} + \frac{X_{\text{AP}}}{1 - X_{\text{AP}}} \left(\frac{W_m}{2} \cdot \frac{(p_{\text{AP}}^{\text{MLD}})^m}{1 - p_{\text{AP}}^{\text{MLD}}} \right) \right. \\ \left. + \sum_{i=0}^{m-1} \frac{W_i \cdot (p_{\text{AP}}^{\text{MLD}})^i}{W_i - 1} + \frac{W_m}{W_m - 1} \cdot \frac{(p_{\text{AP}}^{\text{MLD}})^m}{1 - p_{\text{AP}}^{\text{MLD}}} \right], \quad (27)$$

$$\lambda_2 := \left[\frac{W_0 + 1}{2} + \frac{W_m + 1}{2} \frac{(p_{\text{AP}}^{\text{SLD}})^m}{1 - p_{\text{AP}}^{\text{SLD}}} + \sum_{i=1}^{m-1} \frac{W_i + 1}{2} (p_{\text{AP}}^{\text{SLD}})^i \right]. \quad (28)$$

Then, applying Eq. (9) to the above leads to

$$b_{0,0}^{\text{SLD}} = \left[\lambda_1 \frac{\gamma}{1 - \gamma} + \lambda_2 \right]^{-1}, \quad b_{0,0}^{\text{MLD}} = \left[\lambda_1 + \frac{1 - \gamma}{\gamma} \lambda_2 \right]^{-1}.$$

B. Derivation of transmit probabilities

We are now ready to derive the transmit probability of an AP MLD towards a Non-AP MLD STA and a legacy STA, denoted by $\tau_{\text{AP}}^{\text{MLD}}$ and $\tau_{\text{AP}}^{\text{SLD}}$ respectively, such as

$$\tau_{\text{AP}}^{\text{MLD}} = \sum_{i=0}^m b_{i,0}^{\text{MLD}} = \frac{b_{0,0}^{\text{MLD}}}{1 - p_{\text{AP}}^{\text{MLD}}} = \frac{1/(1 - p_{\text{AP}}^{\text{MLD}})}{\lambda_1 + \frac{1 - \gamma}{\gamma} \lambda_2}, \quad (29)$$

$$\tau_{\text{AP}}^{\text{SLD}} = \sum_{i=0}^m b_{i,0}^{\text{SLD}} = \frac{b_{0,0}^{\text{SLD}}}{1 - p_{\text{AP}}^{\text{SLD}}} = \frac{1/(1 - p_{\text{AP}}^{\text{SLD}})}{\lambda_1 + \frac{\gamma}{1 - \gamma} \lambda_2}. \quad (30)$$

IV. PROPOSED MARKOV CHAIN FOR NON-AP MLD

To better explain our proposed MC in this section, suppose a non-AP MLD's backoff counter for Link 2 reaches zero first and then it is waiting until Link 1's backoff counter also reaches zero. While Link 2 is waiting, it becomes busy and later on Link 1's backoff counter reaches zero, as depicted in Fig. 7. In such a case, the standard mandates that the backoff

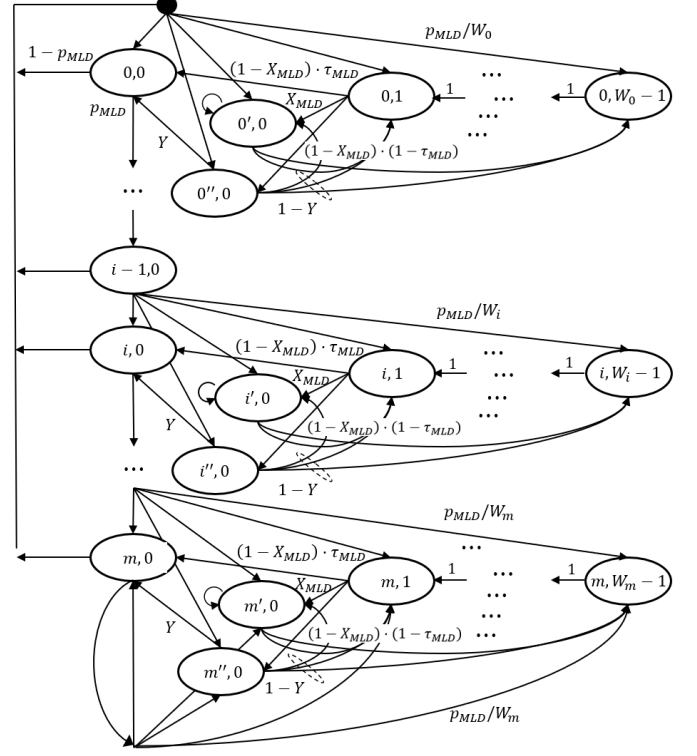


Fig. 9. The proposed MC for the non-AP MLD

process should restart on Link 1 maintaining the same backoff stage. Nevertheless, the start-time alignment model proposed in [14] failed to account for such possibility, leading to inaccuracy under saturated conditions due to frequent channel state changes.

To address this issue in the non-AP MLD MC, we introduce a new state $(i', 0)$ and a state transition from $(i, 1)$ to $(i', 0)$, to allow the backoff process to restart when the backoff counter reaches zero, provided that the other channel busy. Additionally, to accurately model start-time alignment, we introduce another state $(i'', 0)$ and a state transition from $(i, 1)$ to $(i'', 0)$ for the situation where one link's backoff counter reaches zero while the other link's backoff counter has not yet done so. In this case, the link with a zero backoff counter enters $(i'', 0)$ and stays there as long as both links are idle. If either link becomes busy during this waiting period, however, the backoff restarts while retaining the current backoff stage (by making a transition from $(i'', 0)$ to either $(i', 0)$, $(i, 1)$, ..., or $(i, W_i - 1)$); if both links remain idle until the other link's backoff counter also reaches zero, the transmission proceeds (by making a transition from $(i'', 0)$ to $(i, 0)$).

Fig. 8 illustrates the aforementioned mechanism. In the figure, X_{MLD} represents the probability that the other link is busy by other devices and Y denotes the probability that a specific link's backoff counter remains at zero until the other link's backoff counter reaches zero. Building upon the above, the structure of our proposed MC for each non-AP MLD is illustrated in Fig. 9.

A. Derivation of stationary probabilities

In this section, we derive the stationary probabilities of the non-AP MLD's MC in Fig. 9, which are denoted by $b_{i,k}$. After deriving $b_{i,k}$'s, we will present how to derive the two transmit probabilities τ_{MLD}^I and τ_{MLD}^{II} , using p_{MLD}^I and p_{MLD}^{II} respectively. Note that earlier in Section III we distinguished Case 1 from Case 2 according to the packet destination, with two types of transmission probabilities $\tau_{\text{AP}}^{\text{SLD}}$ and $\tau_{\text{AP}}^{\text{MLD}}$. The structure of the non-AP MLD's MC, however, remains unchanged whether the system operates under Case 1 or Case 2, and thus the derivation steps in the sequel would be identical for both cases. In such a vein, we will use the notations τ_{MLD} and p_{MLD} without specifying the corresponding case with a superscript like I or II .²

First, the vertical state transitions among the leftmost states $(i, 0)$, $0 \leq i \leq m$ provide

$$b_{i-1,0} \cdot p_{\text{MLD}} = b_{i,0}, \quad 0 < i < m, \\ \Rightarrow b_{i,0} = p_{\text{MLD}}^i \cdot b_{0,0}, \quad 0 \leq i < m, \quad (31)$$

$$b_{m-1,0} \cdot p_{\text{MLD}} = (1 - p_{\text{MLD}}) \cdot b_{m,0} \\ \Rightarrow b_{m,0} = \frac{(p_{\text{MLD}})^m}{1 - p_{\text{MLD}}} \cdot b_{0,0}, \quad (32)$$

By Eqs. (31) and (32), we obtain

$$\sum_{i=0}^m b_{i,0} = \frac{1 - (p_{\text{MLD}})^m}{1 - p_{\text{MLD}}} \cdot b_{0,0} + \frac{(p_{\text{MLD}})^m}{1 - p_{\text{MLD}}} \cdot b_{0,0} = \frac{b_{0,0}}{1 - p_{\text{MLD}}}. \quad (33)$$

Recall from Section II that a non-AP MLD must align both start and end times to avoid IDC interference. When one link's backoff counter reaches zero, it holds until the other link also reaches zero. If a busy channel is sensed during this period, the link with a zero backoff counter restarts its backoff. To incorporate this behavior into the MC model, we define two probabilities X_{MLD} and Y . First, X_{MLD} is 'the probability that from the viewpoint of a certain link belonging to a non-AP MLD, the other link is busy due to the transmission either from AP MLD, legacy STA or other non-AP MLDs'. In addition, Y represents 'the probability that, within a non-AP MLD, a specific link's backoff counter remains at zero until the other link's backoff counter reaches zero as well'.³ Although X_{MLD} remains unchanged regardless of Case 1 or Case 2, Y could vary, and hence Y_{case_1} must be used when deriving τ_{MLD}^I whereas Y_{case_2} must be used when deriving τ_{MLD}^{II} . Nevertheless, due to the same reason previously explained for τ_{MLD} and p_{MLD} , we will use the notation Y without explicitly differentiating between Y_{case_1} and Y_{case_2} in the sequel.

For stage 0 (i.e., $i = 0$), transitions to/from each state gives

$$b_{0,k} = \frac{W_0 - k}{W_0} \{b_{0,0} + b_{0',0} + (1 - Y)b_{0'',0}\}, \\ 1 \leq k \leq W_0 - 1, \quad (34)$$

by applying g.g.b.e. to each $b_{0,k}$.

²It should be emphasized that p_{MLD}^I should be used when deriving τ_{MLD}^I , whereas p_{MLD}^{II} should be used when deriving τ_{MLD}^{II} .

³Similar to X_{AP} , the derivations of X_{MLD} and Y require τ 's and p 's and thus will be presented later in Section V-D.

Moreover, the state transitions to/from the state $(0', 0)$ gives

$$b_{0',0} = \frac{1}{W_0} \cdot X_{\text{MLD}} \cdot (1 - p_{\text{MLD}}) \cdot \sum_{i=0}^m b_{i,0} + \frac{1}{W_0} \cdot b_{0',0} \\ + \frac{1}{W_0} (1 - Y) \cdot b_{0'',0} + X_{\text{MLD}} \cdot b_{0,1}, \quad (35)$$

to which we apply Eq. (34) to obtain

$$b_{0',0} = \left(\frac{1}{W_0 - 1} + X_{\text{MLD}} \right) \cdot \frac{1 - Y}{1 - X_{\text{MLD}}} \cdot b_{0'',0} \\ + \frac{X_{\text{MLD}}}{1 - X_{\text{MLD}}} \cdot \frac{W_0}{W_0 - 1} \cdot b_{0,0}. \quad (36)$$

Furthermore, the state transitions to/from the state $(0'', 0)$ provides

$$b_{0'',0} = (1 - X_{\text{MLD}}) \cdot (1 - \tau_{\text{MLD}}) \cdot \frac{1}{W_0} \cdot (1 - p_{\text{MLD}}) \cdot \sum_{i=0}^m b_{i,0} \\ + (1 - X_{\text{MLD}}) \cdot (1 - \tau_{\text{MLD}}) \cdot b_{0,1}, \quad (37)$$

to which we can apply Eq. (34) to obtain

$$b_{0'',0} = \frac{(1 - \tau_{\text{MLD}})}{\{1 - (1 - \tau_{\text{MLD}})(1 - Y)\}} \cdot b_{0,0}. \quad (38)$$

Then, by applying Eq. (38) to (36) leads to

$$b_{0',0} = \left[\frac{X_{\text{MLD}}}{1 - X_{\text{MLD}}} \cdot \frac{W_0}{W_0 - 1} + \left(\frac{1}{W_0 - 1} + X_{\text{MLD}} \right) \lambda_3 \right] b_{0,0}, \quad (39)$$

where

$$\lambda_3 := \frac{1 - \tau_{\text{MLD}}}{1 - (1 - \tau_{\text{MLD}})(1 - Y)} \cdot \frac{1 - Y}{1 - X_{\text{MLD}}}. \quad (40)$$

By combining Eqs. (34), (38) and (39), we obtain

$$b_{0,k} = \frac{W_0 - k}{W_0} \cdot \left[1 + \frac{W_0}{W_0 - 1} \left(\frac{X_{\text{MLD}}}{1 - X_{\text{MLD}}} + \lambda_3 \right) \right] \cdot b_{0,0}, \\ 1 \leq k \leq W_0 - 1. \quad (41)$$

Next, for stage m (i.e., $i = m$), the state transitions yield

$$b_{m,k} = \frac{W_m - k}{W_m} \left[\frac{(p_{\text{MLD}})^m}{1 - p_{\text{MLD}}} b_{0,0} + b_{m',0} + (1 - Y)b_{m'',0} \right], \\ 1 \leq k \leq W_m - 1. \quad (42)$$

Then, the state transitions to/from the state $(m', 0)$ gives

$$b_{m',0} = \frac{p_{\text{MLD}}}{W_m} \cdot X_{\text{MLD}} \cdot b_{m-1,0} + \frac{p_{\text{MLD}}}{W_m} \cdot X_{\text{MLD}} \cdot b_{m,0} \\ + \frac{1}{W_m} \cdot b_{m'',0} + \frac{1}{W_m} \cdot (1 - Y) \cdot b_{m'',0} + X_{\text{MLD}} \cdot b_{m,1},$$

to which we can apply Eq. (42) to obtain

$$b_{m',0} = \frac{X_{\text{MLD}}}{1 - X_{\text{MLD}}} \cdot \frac{W_m}{W_{m-1}} \cdot \frac{(p_{\text{MLD}})^m}{1 - p_{\text{MLD}}} b_{0,0} \\ + \frac{1 - Y}{1 - X_{\text{MLD}}} \left(\frac{1}{W_{m-1}} \cdot b_{m'',0} + X_{\text{MLD}} \cdot b_{m',0} \right). \quad (43)$$

Also, by considering the state transitions to/from the state $(m'', 0)$,

$$b_{m'',0} = (1 - X_{\text{MLD}}) \cdot (1 - \tau_{\text{MLD}}) \cdot \left\{ \frac{p_{\text{MLD}}}{W_m} \cdot (b_{m-1,0} + b_{m,0}) + b_{m,1} \right\}, \quad (44)$$

to which we can also apply Eq. (42), leading to

$$b_{m'',0} = \frac{1 - \tau_{\text{MLD}}}{1 - (1 - \tau_{\text{MLD}})(1 - Y)} \cdot \frac{(p_{\text{MLD}})^m}{1 - p_{\text{MLD}}} \cdot b_{0,0}. \quad (45)$$

Then, applying Eq. (45) to Eq. (43) provides

$$b_{m',0} = \left[\frac{X_{\text{MLD}}}{1 - X_{\text{MLD}}} \cdot \frac{W_m}{W_{m-1}} + \frac{1}{W_{m-1}} \cdot \lambda_3 \right] \frac{(p_{\text{MLD}})^m}{1 - p_{\text{MLD}}} \cdot b_{0,0} + X_{\text{MLD}} \cdot \lambda_3 \cdot \frac{(p_{\text{MLD}})^m}{1 - p_{\text{MLD}}} \cdot b_{0,0}. \quad (46)$$

By combining Eqs. (42), (45), and (46),

$$b_{m,k} = \frac{W_m - k}{W_m} \cdot \frac{(p_{\text{MLD}})^m}{1 - p_{\text{MLD}}} \cdot \left[1 + \frac{X_{\text{MLD}}}{1 - X_{\text{MLD}}} \cdot \frac{W_m}{W_{m-1}} + \frac{W_m}{W_{m-1}} \cdot \lambda_3 \right] \cdot b_{0,0}, \quad 1 \leq k \leq W_m - 1, \\ b_{m,0} = \frac{(p_{\text{MLD}})^m}{1 - p_{\text{MLD}}} \cdot b_{0,0}, \quad k = 0.$$

Following the procedures above similarly, the state transitions at each state for $1 \leq i \leq m - 1$ provide

$$b_{i,k} = \frac{W_i - k}{W_i} \left\{ (p_{\text{MLD}})^i \cdot b_{0,0} + b_{i',0} + (1 - Y) \cdot b_{i'',0} \right\}, \quad 1 \leq k \leq W_i - 1. \quad (47)$$

Next, the state transitions to/from the state $(i', 0)$ provide

$$b_{i',0} = \frac{p_{\text{MLD}}}{W_i} \cdot X_{\text{MLD}} \cdot b_{i-1,0} + \frac{1}{W_i} \cdot b_{i',0} + \frac{1}{W_i} \cdot (1 - Y) \cdot b_{i'',0} + X_{\text{MLD}} \cdot b_{i,1},$$

to which we can apply Eq. (47) to obtain

$$b_{i',0} = \frac{1}{W_{i-1}} \cdot \frac{1 - Y}{1 - X_{\text{MLD}}} \cdot b_{i'',0} + \frac{X_{\text{MLD}} \cdot (1 - Y)}{1 - X_{\text{MLD}}} \cdot b_{i'',0} + \frac{X_{\text{MLD}}}{1 - X_{\text{MLD}}} \cdot \frac{W_i}{W_{i-1}} \cdot (p_{\text{MLD}})^i \cdot b_{0,0}. \quad (48)$$

In addition, the state transitions to/from the state $(i'', 0)$ provide

$$b_{i'',0} = \frac{1 - \tau_{\text{MLD}}}{1 - (1 - \tau_{\text{MLD}})(1 - Y)} \cdot (p_{\text{MLD}})^i \cdot b_{0,0}. \quad (49)$$

Then by applying Eq. (49) to Eq. (48), we obtain

$$b_{i',0} = \left[\frac{X_{\text{MLD}}}{1 - X_{\text{MLD}}} \cdot \frac{W_i}{W_{i-1}} + \frac{\lambda_3}{W_{i-1}} + X_{\text{MLD}} \lambda_3 \right] (p_{\text{MLD}})^i b_{0,0}. \quad (50)$$

By combining Eqs. (47), (49), and (50),

$$b_{i,k} = \frac{W_i - k}{W_i} \left\{ 1 + \frac{W_i}{W_{i-1}} \left(\frac{X_{\text{MLD}}}{1 - X_{\text{MLD}}} + \lambda_3 \right) \right\} (p_{\text{MLD}})^i b_{0,0}, \quad 1 \leq k \leq W_i - 1, \\ b_{i,0} = (p_{\text{MLD}})^i \cdot b_{0,0}, \quad k = 0. \quad (51)$$

Since the sum of stationary probabilities should be 1, we get

$$1 = \sum_{i=0}^m \sum_{k=0}^{W_i-1} b_{i,k} + \sum_{i'=0'}^{m'} b_{i',0} + \sum_{i''=0''}^{m''} b_{i'',0} = \sum_{k=0}^{W_0-1} b_{0,k} + \sum_{k=0}^{W_m-1} b_{m,k} + \sum_{i=1}^{m-1} \sum_{k=0}^{W_i-1} b_{i,k} + \sum_{i'=0'}^{m'} b_{i',0} + \sum_{i''=0''}^{m''} b_{i'',0}. \quad (52)$$

By applying Eqs. (38) through (51) to the above, we obtain

$$1 = \left[\frac{1}{1 - p_{\text{MLD}}} + \left\{ \frac{W_0 - 1}{2} + \frac{X_{\text{MLD}}}{1 - X_{\text{MLD}}} \cdot \frac{W_0}{2} + \frac{W_0}{2} \cdot \lambda_3 \right\} \frac{(p_{\text{MLD}})^m}{1 - p_{\text{MLD}}} + \left\{ \frac{W_m - 1}{2} + \frac{X_{\text{MLD}}}{1 - X_{\text{MLD}}} \cdot \frac{W_m}{2} + \frac{W_m}{2} \cdot \lambda_3 \right\} \frac{(p_{\text{MLD}})^m}{1 - p_{\text{MLD}}} + \sum_{i=1}^{m-1} \sum_{k=1}^{W_i-1} \left\{ \frac{W_i - k}{W_i} + \frac{W_i - k}{W_i - 1} \left(\frac{X_{\text{MLD}}}{1 - X_{\text{MLD}}} + \lambda_3 \right) \right\} p^i + \sum_{i=0}^{m-1} \left\{ \frac{1}{W_i - 1} \left(\frac{X_{\text{MLD}} \cdot W_i}{1 - X_{\text{MLD}}} + \lambda_3 \right) + X_{\text{MLD}} \lambda_3 \right\} (p_{\text{MLD}})^i + \left\{ \frac{1}{W_m - 1} \left(\frac{X_{\text{MLD}} \cdot W_m}{1 - X_{\text{MLD}}} + \lambda_3 \right) + X_{\text{MLD}} \lambda_3 \right\} \frac{(p_{\text{MLD}})^m}{1 - p_{\text{MLD}}} + \frac{\lambda_3}{1 - p_{\text{MLD}}} \cdot \frac{1 - X_{\text{MLD}}}{1 - Y} \right] \cdot b_{0,0}. \quad (53)$$

B. Derivation of transmit probabilities

We are now ready to derive the transmit probability of a non-AP MLD STA towards the AP MLD, denoted by τ_{MLD} , which is given as

$$\tau_{\text{MLD}} = \sum_{i=0}^m b_{i,0} = \frac{b_{0,0}}{1 - p_{\text{MLD}}}, \quad (54)$$

where $b_{0,0}$ can be obtained from Eq. (53).

V. DERIVATION OF KEY PARAMETERS IN THE PROPOSED MARKOV CHAINS

A. Transmit probabilities of SLD

For legacy devices, the transmit probability τ_{SLD} can be derived from the Bianchi model in [17], [18]. Considering that τ_{SLD} is influenced by the destination of an AP MLD's transmitted packet (Case 1 or Case 2), we derive τ_{SLD} for each case as follows:

$$\tau_{\text{SLD}}^I = \left[\frac{1 - p_{\text{SLD}}^I - p_{\text{SLD}}^I (2p_{\text{SLD}}^I)^m}{1 - 2p_{\text{SLD}}^I} \cdot \frac{(CW_{\min}^{\text{SLD}} + 1)}{2} + \frac{1}{2} \right]^{-1}, \\ \tau_{\text{SLD}}^{II} = \left[\frac{1 - p_{\text{SLD}}^{II} - p_{\text{SLD}}^{II} (2p_{\text{SLD}}^{II})^m}{1 - 2p_{\text{SLD}}^{II}} \cdot \frac{(CW_{\min}^{\text{SLD}} + 1)}{2} + \frac{1}{2} \right]^{-1},$$

where CW_{\min}^{SLD} is the minimum contention window size employed by the legacy devices.

B. Collision probabilities of AP MLD, non-AP MLD, SLD

We derive the *collision* probability p , per device and per slot, using the derived τ 's for Case 1 and Case 2. For Case 1, the collision probabilities of an AP MLD, a non-AP MLD, and an SLD are denoted by p_{AP}^{SLD} , p_{MLD}^I , and p_{SLD}^I , respectively, which can be derived as

$$\begin{aligned} p_{AP}^{SLD} &= 1 - (1 - \tau_{SLD}^I)^{N_{SLD}} (1 - \tau_{MLD}^I)^{N_{MLD}}, \\ p_{MLD}^I &= 1 - (1 - \tau_{AP}^{SLD}) (1 - \tau_{SLD}^I)^{N_{SLD}} (1 - \tau_{MLD}^I)^{N_{MLD}-1}, \\ p_{SLD}^I &= 1 - (1 - \tau_{AP}^{SLD}) (1 - \tau_{SLD}^I)^{N_{SLD}-1} (1 - \tau_{MLD}^I)^{N_{MLD}}. \end{aligned}$$

Similarly, the collision probabilities of an AP MLD, a non-AP MLD, and an SLD in Case 2 are denoted by p_{AP}^{MLD} , p_{MLD}^{II} , and p_{SLD}^{II} , respectively, which are derived as

$$\begin{aligned} p_{AP}^{MLD} &= 1 - (1 - \tau_{SLD}^{II})^{N_{SLD}} (1 - \tau_{MLD}^{II})^{N_{MLD}}, \\ p_{MLD}^{II} &= 1 - (1 - \tau_{AP}^{MLD}) (1 - \tau_{SLD}^{II})^{N_{SLD}} (1 - \tau_{MLD}^{II})^{N_{MLD}-1}, \\ p_{SLD}^{II} &= 1 - (1 - \tau_{AP}^{MLD}) (1 - \tau_{SLD}^{II})^{N_{SLD}-1} (1 - \tau_{MLD}^{II})^{N_{MLD}}. \end{aligned}$$

Next, we derive the probability of every possible event occurring in a random slot, using τ 's and p 's. In Case 1, the probability p_{idle}^I that no one transmits in a slot is derived as

$$p_{idle}^I = (1 - \tau_{AP}^{SLD}) (1 - \tau_{SLD}^I)^{N_{SLD}} (1 - \tau_{MLD}^I)^{N_{MLD}}.$$

The probability τ_1^I that the AP MLD alone transmits a packet destined to a legacy STA is derived as

$$\tau_1^I = \tau_{AP}^{MLD} \cdot (1 - p_{AP}^{SLD}).$$

The probability τ_2^I that a legacy device alone transmits (to the AP) is derived as

$$\tau_2^I = N_{SLD} \cdot \tau_{SLD}^I \cdot (1 - p_{SLD}^I).$$

The probability τ_3^I that a non-AP MLD alone transmits (to the AP) is derived as

$$\tau_3^I = N_{MLD} \cdot \tau_{MLD}^I \cdot (1 - p_{MLD}^I).$$

The collision probability $p_{c,1}^I$ between AP MLD's DL transmission to a legacy device and one or more UL transmissions from non-AP MLDs and/or legacy devices is derived as

$$p_{c,1}^I = \tau_{AP}^{SLD} \cdot p_{AP}^{SLD}.$$

The collision probability $p_{c,2}^I$ between non-AP MLDs and legacy devices is derived as

$$p_{c,2}^I = 1 - p_{idle}^I - (\tau_1^I + \tau_2^I + \tau_3^I) - p_{c,1}^I.$$

In Case 2, the aforementioned p_{idle}^I , τ_2^I , τ_3^I , $p_{c,1}^I$, and $p_{c,2}^I$ are re-denoted by p_{idle}^{II} , τ_2^{II} , τ_3^{II} , $p_{c,1}^{II}$, and $p_{c,2}^{II}$, respectively, where they can be derived similar to Case 1 but using Case 2's τ and p . On the other hand, when the AP MLD alone transmits a packet to a non-AP MLD, we need to consider two different cases. First, the AP MLD can transmit either through a single link to the non-AP MLD or through both links to a couple of non-AP MLDs, with probability τ_{1a}^{II} , which is derived as

$$\tau_{1a}^{II} = \left(1 - \frac{1}{N_{MLD}} \cdot \tau_{AP}^{MLD}\right) \cdot \tau_{AP}^{MLD},$$

where $1/N_{MLD}$ represents the probability that in case both links are used, the destination of the two packets is the same

non-AP MLD. Second, the AP MLD may transmit alone through both links while its destination is the same non-AP MLD, with probability τ_{1b}^{II} , which is derived as

$$\tau_{1b}^{II} = \frac{1}{N_{MLD}} \cdot \tau_{AP}^{MLD} \cdot \tau_{AP}^{MLD}.$$

Then, the other probabilities can be expressed as

$$\begin{aligned} p_{idle}^{II} &= (1 - \tau_{AP}^{MLD}) \cdot (1 - \tau_{SLD}^{II})^{N_{SLD}} \cdot (1 - \tau_{MLD}^{II})^{N_{MLD}}, \\ \tau_2^{II} &= N_{SLD} \cdot \tau_{SLD}^{II} \cdot (1 - \tau_{AP}^{MLD}) \cdot (1 - \tau_{SLD}^{II})^{N_{SLD}-1} \\ &\quad \cdot (1 - \tau_{MLD}^{II})^{N_{MLD}}, \\ \tau_3^{II} &= N_{MLD} \cdot \tau_{MLD}^{II} \cdot (1 - \tau_{AP}^{MLD}) \cdot (1 - \tau_{SLD}^{II})^{N_{SLD}} \\ &\quad \cdot (1 - \tau_{MLD}^{II})^{N_{MLD}-1}, \\ p_{c,1}^{II} &= \tau_{AP}^{MLD} \cdot p_{AP}^{MLD}, \\ p_{c,2}^{II} &= 1 - (p_{idle}^{II} + b_3) - (\tau_{1a}^{II} + \tau_{1b}^{II} + \tau_2^{II} + \tau_3^{II}) - p_{c,1}^{II}. \end{aligned}$$

C. Duration of each event in a random slot

Each aforementioned event has a corresponding time duration. We briefly explain how these durations are derived. We assume that all transmissions are based on Aggregated MPDUs (A-MPDU), and all devices use the same modulation coding scheme (MCS) index. Then, the time T_{data} required for data transmission is given as

$$T_{data} = T_{PHY} + \lceil L_{AMPDU}/r_{SU} \rceil \cdot \sigma \quad (55)$$

where T_{PHY} is the duration of PHY preamble and header, L_{AMPDU} is the length of both DL and UL packets, r_{SU} is the data rate (bits/symbol), and σ is the OFDM symbol duration given by [18]. With T_{data} given, the time $T_{success}$ to take for a successful transmission is derived as

$$T_{success} = T_{DATA} + SIFS + T_{ACK} + SIFS, \quad (56)$$

where T_{ACK} is the ACK frame duration. Then, the duration $T_{collision}$ of collision is derived as

$$T_{collision} = T_{DATA} + SIFS. \quad (57)$$

As a result, the time duration for each event is as follows: $T_{\tau_1^I} = T_{\tau_2^I} = \dots = T_{\tau_3^{II}} = T_{success}$ and $T_{p_{c,1}^I} = T_{p_{c,2}^I} = \dots = T_{p_{c,2}^{II}} = T_{collision}$. Then, we can calculate the average duration ϕ considering all the events including successful transmission, collision, and an empty slot as follows:

$$\begin{aligned} \phi_{case1} &= p_{idle}^I \cdot T_{empty} + (\tau_1^I + \tau_2^I + \tau_3^I) (T_{success} + T_{empty}) \\ &\quad + (p_{c,1}^I + p_{c,2}^I) (T_{collision} + T_{empty}), \quad (58) \\ \phi_{case2} &= p_{idle}^{II} \cdot T_{empty} + (\tau_{1a}^{II} + \tau_{1b}^{II} + \tau_2^{II} + \tau_3^{II}) (T_{success} \\ &\quad + T_{empty}) + (p_{c,1}^{II} + p_{c,2}^{II}) (T_{collision} + T_{empty}), \quad (59) \end{aligned}$$

where T_{empty} is the empty slot duration.

D. Derivation of X_{AP} , X_{MLD} , and Y

In Section III and Section IV, the definitions of X_{AP} , X_{MLD} and Y were provided when deriving τ_{AP} and τ_{MLD} . We hereby derive X_{AP} , X_{MLD} , and Y , by utilizing the parameters derived earlier in this section.

First, remind that X_{AP} is the probability that from the viewpoint of a certain link belonging to the AP MLD, the other link is busy due to the transmission either from non-AP MLD or legacy STA. Accordingly, X_{AP} can be obtained by considering the proportion of time in a slot where the channel is busy due to the transmission from either non-AP MLD or legacy STA. For Case 1, the duration $\phi_{\text{busy}}^{\text{AP},I}$ per slot when the other link is busy due to the transmission by non-AP MLD or legacy STA is given as

$$\phi_{\text{busy}}^{\text{AP},I} = \phi_{\text{case1}} - T_{\text{idle}}^I - \tau_{\text{AP}}^{\text{SLD}} \cdot (1 - p_{\text{AP}}^{\text{SLD}}) \cdot T_{\text{success}} - \tau_{\text{AP}}^{\text{SLD}} \cdot p_{\text{AP}}^{\text{SLD}} \cdot T_{\text{collision}}, \quad (60)$$

$$T_{\text{idle}}^I = p_{\text{idle}}^I \cdot T_{\text{empty}}, \quad (61)$$

where T_{idle}^I implies the period that the channel is idle per slot in Case 1. Similarly, $\phi_{\text{busy}}^{\text{AP},II}$ and T_{idle}^{II} for Case 2 are given as

$$\phi_{\text{busy}}^{\text{AP},II} = \phi_{\text{case2}} - T_{\text{idle}}^{II} - \tau_{\text{AP}}^{\text{MLD}} \cdot (1 - p_{\text{AP}}^{\text{MLD}}) \cdot T_{\text{success}} - \tau_{\text{AP}}^{\text{MLD}} \cdot p_{\text{AP}}^{\text{MLD}} \cdot T_{\text{collision}}, \quad (62)$$

$$T_{\text{idle}}^{II} = p_{\text{idle}}^{II} \cdot T_{\text{empty}}. \quad (63)$$

For a link, the other link is in Case 1 with probability $(1 - \gamma)$ and in Case 2 with probability γ , and thus we obtain X_{AP} as

$$X_{AP} = (1 - \gamma) \cdot \frac{\phi_{\text{busy}}^{\text{AP},I}}{\phi_{\text{case1}}} + \gamma \cdot \frac{\phi_{\text{busy}}^{\text{AP},II}}{\phi_{\text{case2}}}.$$

Next, X_{MLD} is the probability that from the perspective of a link belonging to a non-AP MLD, the other link is busy due to the transmission either from the AP MLD, legacy devices, or other non-AP MLDs. This can be obtained by excluding the periods when no transmission occurs, when a single non-AP MLD transmits, when the AP and a non-AP MLD transmit simultaneously resulting in a collision, and when the AP does not transmit but a collision occurs between a non-AP MLD and other devices. Specifically, in Case 1, the duration per slot $\phi_{\text{busy}}^{\text{MLD},I}$ when the other link is busy due to the transmission by the devices *excluding* one non-AP MLD is given as

$$\begin{aligned} \phi_{\text{busy}}^{\text{MLD},I} &= \phi_{\text{case1}} - T_{\text{idle}}^I - \tau_{\text{MLD}}^I \cdot (1 - p_{\text{MLD}}^I) \cdot T_{\text{success}} \\ &\quad - \tau_{\text{AP}}^{\text{SLD}} \cdot \tau_{\text{MLD}}^I \cdot T_{\text{collision}} - (1 - \tau_{\text{AP}}^{\text{SLD}}) \cdot \tau_{\text{MLD}}^I \\ &\quad \cdot (1 - (1 - \tau_{\text{MLD}}^I)^{N-1} \cdot (1 - \tau_{\text{legacy}}^I)^N) \cdot T_{\text{collision}}. \end{aligned} \quad (64)$$

Similarly, $\phi_{\text{busy}}^{\text{MLD},II}$ for Case 2 is derived as

$$\begin{aligned} \phi_{\text{busy}}^{\text{MLD},II} &= \phi_{\text{case2}} - T_{\text{idle}}^{II} - \tau_{\text{MLD}}^{II} \cdot (1 - p_{\text{MLD}}^{II}) \cdot T_{\text{success}} \\ &\quad - \tau_{\text{AP}}^{\text{MLD}} \cdot \tau_{\text{MLD}}^{II} \cdot T_{\text{collision}} - (1 - \tau_{\text{AP}}^{\text{MLD}}) \cdot \tau_{\text{MLD}}^{II} \\ &\quad \cdot (1 - (1 - \tau_{\text{MLD}}^{II})^{N-1} \cdot (1 - \tau_{\text{legacy}}^{II})^N) \cdot T_{\text{collision}}. \end{aligned} \quad (65)$$

Then we obtain X_{MLD} as

$$X_{MLD} = (1 - \gamma) \cdot \frac{\phi_{\text{busy}}^{\text{MLD},I}}{\phi_{\text{case1}}} + \gamma \cdot \frac{\phi_{\text{busy}}^{\text{MLD},II}}{\phi_{\text{case2}}}.$$

Finally, Y denotes the probability that, within a non-AP MLD, one link's backoff counter remains at zero until the other link's backoff counter also reaches zero. Without loss of generality, assuming Link 1 is currently in $(i'', 0)$, suppose Link 2's backoff counter is j ($j \neq 0$). Then, if both Link 1 and Link 2 remain idle for j slots, Link 2's backoff counter will reach zero thus allowing simultaneous transmissions at both links (which corresponds to $(i'', 0) \rightarrow (i, 0)$ transition in Fig. 9). Therefore, when Link 1 is in Case 1, Y_{case1} is derived as

$$\begin{aligned} Y_{\text{case1}} &= \sum_{i''=0}^m \sum_{j=1}^{W_0-1} \sum_{i=0}^m b_{i'',0}^I \cdot (p_{\text{idle}}^I)^j \\ &\quad \cdot \{ (1 - \gamma) \cdot b_{i,j}^I \cdot (p_{\text{idle}}^I)^j + \gamma \cdot b_{i,j}^{II} \cdot (p_{\text{idle}}^{II})^j \} \\ &\quad + \sum_{k=1}^m \sum_{i''=k}^m \sum_{j=W_{i''-1}}^{W_{i''}-1} \sum_{i=k}^m b_{i'',0}^I \cdot (p_{\text{idle}}^I)^j \\ &\quad \cdot \{ (1 - \gamma) \cdot b_{i,j}^I \cdot (p_{\text{idle}}^I)^j + \gamma \cdot b_{i,j}^{II} \cdot (p_{\text{idle}}^{II})^j \}. \end{aligned} \quad (66)$$

In addition, when Link 1 is in Case 2, Y_{case2} is given as

$$\begin{aligned} Y_{\text{case2}} &= \sum_{i''=0}^m \sum_{j=1}^{W_0-1} \sum_{i=0}^m b_{i'',0}^{II} \cdot (p_{\text{idle}}^{II})^j \\ &\quad \cdot \{ (1 - \gamma) \cdot b_{i,j}^I \cdot (p_{\text{idle}}^I)^j + \gamma \cdot b_{i,j}^{II} \cdot (p_{\text{idle}}^{II})^j \} \\ &\quad + \sum_{k=1}^m \sum_{i''=k}^m \sum_{j=W_{i''-1}}^{W_{i''}-1} \sum_{i=k}^m b_{i'',0}^{II} \cdot (p_{\text{idle}}^{II})^j \\ &\quad \cdot \{ (1 - \gamma) \cdot b_{i,j}^I \cdot (p_{\text{idle}}^I)^j + \gamma \cdot b_{i,j}^{II} \cdot (p_{\text{idle}}^{II})^j \}. \end{aligned} \quad (67)$$

E. Derivation of per-device per-link throughput

Finally, we derive per-device per-link throughput as follows.
Per-link UL throughput of a legacy device:

$$S_U^{\text{SLD}} = \frac{1}{N_{\text{SLD}}} \cdot \left[(1 - \gamma) \cdot \frac{\tau_2^I}{\phi_{\text{case1}}} + \gamma \cdot \frac{\tau_2^{II}}{\phi_{\text{case2}}} \right] \cdot n_a \cdot L_D, \quad (68)$$

Per-link UL throughput of a non-AP MLD:

$$\begin{aligned} S_U^{\text{MLD}} &= \frac{1}{N_{\text{MLD}}} \cdot \left[(1 - \gamma) \cdot \frac{\tau_3^I}{\phi_{\text{case1}}} \cdot (1 - p_{\text{MLD}}^I)^{N_{th}(p_{\text{MLD}}^I)} \right. \\ &\quad \left. + \gamma \cdot \frac{\tau_3^{II}}{\phi_{\text{case2}}} \cdot (1 - p_{\text{MLD}}^{II})^{N_{th}(p_{\text{MLD}}^{II})} \right] \cdot n_a \cdot L_D, \end{aligned} \quad (69)$$

Per-link DL throughput from AP MLD to a legacy device:

$$S_D^{\text{SLD}} = \frac{\tau_1^I}{\phi_{\text{case1}}} \cdot n_a \cdot L_D, \quad (70)$$

Per-link DL throughput from AP MLD to a non-AP MLD:

$$\begin{aligned} S_D^{\text{MLD}} &= \left[\frac{\tau_{1a}^{II}}{\phi_{\text{case1}}} + \frac{\tau_{1b}^{II}}{\phi_{\text{case2}}} \cdot \left\{ 1 - \frac{N_{th}(p_{\text{AP}}^{\text{MLD}}) \cdot T_{\text{empty}}}{T_{\text{data}}} \right\} \right. \\ &\quad \left. \cdot (1 - p_{\text{AP}}^{\text{MLD}})^{N_{th}(p_{\text{AP}}^{\text{MLD}})} \right] \cdot n_a \cdot L_D, \end{aligned} \quad (71)$$

where n_a is the number of aggregated MPDUs, L_D is the payload length, and $N_{th}(\cdot)$ is the average difference in backoff counter values between two links belonging to an MLD [14].

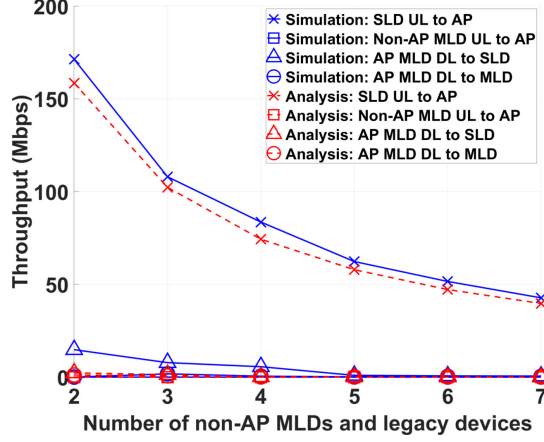


Fig. 10. Per-device throughput when $N_{\text{MLD}} = N_{\text{SLD}}$

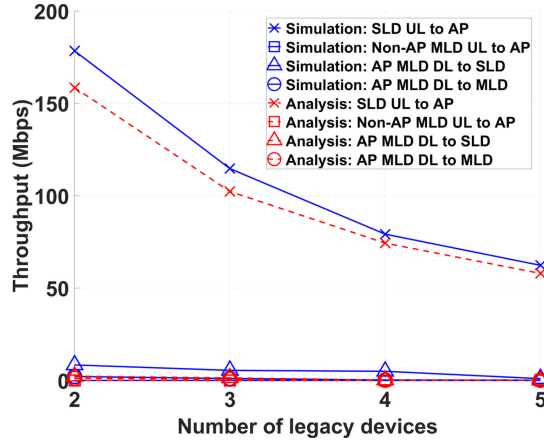


Fig. 11. Per-device throughput when $N_{\text{MLD}} \neq N_{\text{SLD}}$ and $N_{\text{MLD}} = 5$

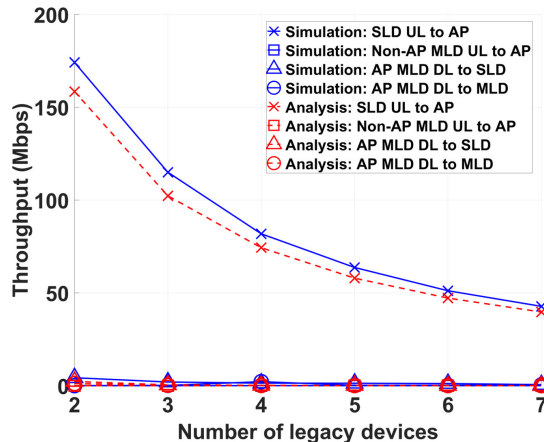


Fig. 12. Per-device throughput when $N_{\text{MLD}} \neq N_{\text{SLD}}$ and $N_{\text{MLD}} = 7$

VI. PERFORMANCE EVALUATION

This section evaluates the accuracy of the proposed analytical framework, and also examines the behavior of MLDs and legacy devices in various coexistence scenarios. For this purpose, we have jointly utilized two discrete-event network simulators, ns-3 [19] and MATLAB [20], where ns-3 is a modular C++ based simulator widely used in the networking field. As of its latest release (ns-3.42), however, only STR is implemented among MLO functionalities, and hence we implemented essential NSTR functionalities in ns-3 to validate our proposed analysis, including start-time alignment, end-time alignment, and other key features proposed in this paper. In addition, to evaluate τ 's and p 's which are iteratively affecting each other as shown in Sections III through V, we utilized MATLAB's Optimization Toolbox and its nonlinear equation solver [21].

As described earlier in Section II, we assume that each MLD has two links at 5 GHz and 6 GHz, respectively, and the network consists of one AP MLD, N_{MLD} non-AP MLDs, and N_{legacy} legacy devices per link. All devices are randomly distributed within the 5-meter radius from the AP and use MCS 8 with 80 MHz channel bandwidth. We also assume the saturated traffic condition, and hence all devices always have packets to transmit where the packet size is 1500 bytes. In addition, each simulation scenario was run for 5 more seconds after every device's queue is sufficiently filled with packets.

Note that while our analytical model focuses on dual-link MLDs, it does not assume symmetric link behaviors at all. Unlike [14], we construct separate per-link MCs to model independent contention/channel dynamics. Such flexibility for heterogeneity has also been reflected in our simulation setup.

A. Per-device throughput when $N_{\text{MLD}} = N_{\text{SLD}}$

First, we compare per-device per-link throughput obtained from our analysis with the one measured by ns-3 simulation, for scenarios with $N_{\text{MLD}} = N_{\text{SLD}}$. Fig. 10 illustrates the throughput trend as N_{MLD} and N_{SLD} increase up to seven. The plots show that all three types of throughput (i.e., SLD's, Non-AP MLD's, and AP MLD's) tend to decrease with N_{MLD} (or equivalently N_{SLD}) due to aggravated competition among the coexisting devices, while the proposed analysis and simulated results closely correspond to each other for each type of devices. Among them, the SLD's (i.e., legacy device's) UL throughput achieves a dominantly large throughput, where the discrepancy between analysis and simulation presents an acceptable level of error varying as [7.4, 5.2, 11.0, 7.0, 8.4, 7.1] (%) for $N_{\text{MLD}} = N_{\text{SLD}} = [2, 3, 4, 5, 6, 7]$ respectively. The AP MLD's DL throughput and the non-AP MLD's UL throughput, however, are evaluated as significantly smaller than the SLD UL throughput, making the comparison between analysis and simulation less meaningful. Nevertheless, all the results confirm that the gap between analysis and simulation gets smaller as the number of non-AP STAs increases, showing the reliability of the proposed analysis even in a larger network.

More specifically, the SLD UL throughput achieves [158.4, 102.2, 74.3, 57.8, 47.1, 39.6] Mbps in analysis and [171.2, 107.9, 83.5, 62.2, 51.5, 42.7] Mbps in simulation. In

the meantime, the non-AP MLD UL throughput remains negligible, ranging from 0.000007 to 0.00247 Mbps across all cases in analysis, while it is consistently measured as 0 Mbps in simulation. For the AP MLD, its DL throughput to an SLD steadily decreases as [2.2, 1.3, 0.1, 0.08, 0.04, 0.03] Mbps in analysis, while the simulation shows [14.7, 7.7, 5.6, 0.9, 0.6, 0.5] Mbps. In addition, the AP MLD's DL throughput to a non-AP MLD presents [1.1, 0.6, 0.08, 0.04, 0.02, 0.01] Mbps in analysis, while showing [0, 1.7, 0.4, 0.1, 0.3, 0.3] Mbps in simulation.

The aforementioned results reveal significant challenges in utilizing MLO in the coexistence scenario with Wi-Fi 7 and legacy Wi-Fi. Employing non-AP MLDs becomes disadvantageous particularly due to its start-time alignment requirement, which mandates that both links have their backoff counters reach zero simultaneously. In saturated conditions, however, all the channels are frequently busy, causing one link to restart its backoff process when the other link switches from idle to busy. As a result, legacy devices may dominate to utilize the channels securing the majority of transmission opportunities, while MLDs are struggling to obtain the chance for transmission. On the other hand, the AP MLD also faces difficulty in transmitting packets to non-AP MLDs. If the AP attempts transmission to a non-AP MLD on one link, it should not proceed if the other link is busy except when its busyness is due to the transmission by the AP itself, so as to prevent potential IDC interference at non-AP MLDs as discussed in Section II. Moreover, saturated conditions exacerbate such a situation, causing the packets destined to non-AP MLDs to remain in the AP MLD's queue, ultimately leading to a reduced DL throughput.

B. Per-device throughput when $N_{\text{MLD}} \neq N_{\text{SLD}}$

To investigate how the system dynamics change when there exist an imbalanced number of MLDs and SLDs, i.e., $N_{\text{MLD}} \neq N_{\text{SLD}}$, we now fix N_{MLD} to 5, and vary the number of legacy devices from 2 to 5. Likewise, we also consider the case with $N_{\text{MLD}} = 7$ and N_{SLD} varies from 2 to 7.

Fig. 11 shows that even when N_{SLD} is fewer than N_{MLD} , the results remain similar to those observed in Fig. 10. More specifically, the SLD UL throughput achieves [158.4, 102.2, 74.3, 57.8] Mbps in analysis and [178.3, 114.6, 79.1, 62.2] Mbps in simulation. In the meantime, the non-AP MLD UL throughput remains negligible, yielding values that are effectively zero in analysis and exactly zero in simulation. For the AP MLD, its DL throughput to an SLD steadily decreases as [2.2, 1.3, 0.1, 0.08] Mbps in analysis, while the simulation shows [8.3, 5.4, 4.9, 0.9] Mbps. In addition, the AP MLD's DL throughput to a non-AP MLD presents [1.1, 0.6, 0.06, 0.04] Mbps in analysis, while showing [2.0, 1.0, 0.2, 0.1] Mbps in simulation.

A notable observation here is that even when legacy devices are less populated than non-AP MLDs, the latter still hardly transmit. This result demonstrates that under saturated conditions, satisfying the start-time alignment requirement becomes really challenging. The same observation can be made for the AP MLD as discussed in Section VI-A, which faces

the challenge in avoiding potential IDC interference. In the meantime, the error between analysis and simulation for the SLD UL throughput is measured as [11.1, 10.7, 6.1, 7.0] (%) for $N_{\text{SLD}} = [2, 3, 4, 5]$ respectively, demonstrating a reasonable level of consistency.

Next, Fig. 12 illustrates the case when $N_{\text{MLD}} = 7$ and N_{SLD} varies from 2 to 7, which allows us to explore whether increasing the number of non-AP MLDs alters the dynamics observed in previous setup. Similar to the previous scenario, the SLD UL throughput dominates the network while the AP MLD DL throughput is significantly smaller and the non-AP MLD UL throughput stays negligible. Particularly, the SLD UL throughput is obtained as [158.4, 102.2, 74.3, 57.9, 47.1, 39.6] Mbps by analysis while the simulation measures slightly higher values of [174.1, 114.9, 81.8, 63.7, 51.1, 42.7] Mbps, presenting the error of [9.0, 11.1, 9.2, 9.1, 7.8, 7.3] (%), still demonstrating a reasonable level of consistency. Such results indicate that under saturated conditions, despite of the further increase in the number of non-AP MLDs, the presence of even a small number of legacy devices prevents both the AP MLD and non-AP MLDs from obtaining meaningful transmission opportunities due to the constraints imposed by NSTR operations.

VII. CONCLUSION

This paper addressed some critical operations of MLO overlooked by existing studies, specifically focusing on the backoff behavior of MLDs as mandated by the standard. In particular, we proposed a series of novel MCs that accurately model the behavior of the standard-compliant AP MLD and non-AP MLDs respectively, and derived their stationary probabilities and closed-form per-device throughputs in the Wi-Fi 7 coexistence scenario.

In future, we would like to leverage on the developed framework to develop more efficient coexistence mechanisms for MLO-based Wi-Fi 7 with legacy WLANs.

REFERENCES

- [1] C. Deng, X. Fang, X. Han, X. Wang, L. Yan, R. He, Y. Long, and Y. Guo, "IEEE 802.11be Wi-Fi 7: New Challenges and Opportunities," *IEEE Communications Surveys & Tutorials*, vol. 22, no. 4, pp. 2136–2166, 2020.
- [2] J. Ssimbwa, S.-H. Yoon, Y. Lee, and Y.-C. Ko, "Towards 5G-Advanced NR-Uncolored Systems: Physical Layer Design and Performance," *Journal of Communications and Networks*, vol. 26, no. 2, pp. 207–214, Apr. 2024.
- [3] A. López-Raventós and B. Bellalta, "Multi-link Operation in IEEE 802.11be WLANs," *IEEE Wireless Communications*, vol. 29, no. 4, pp. 94–100, 2022.
- [4] E. Khorov, I. Levitsky, and I. F. Akyildiz, "Current Status and Directions of IEEE 802.11be, the Future Wi-Fi 7," *IEEE Access*, vol. 8, pp. 88 664–88 688, 2020.
- [5] W. Murti and J.-H. Yun, "Multi-link Operation with Enhanced Synchronous Channel Access in IEEE 802.11be Wireless LANs: Coexistence Issue and Solutions," *Sensors*, vol. 21, no. 23, p. 7974, 2021.
- [6] A. López-Raventós and B. Bellalta, "Dynamic Traffic Allocation in IEEE 802.11be Multi-link WLANs," *IEEE Wireless Communications Letters*, vol. 11, no. 7, pp. 1404–1408, 2022.
- [7] C. Chen, X. Chen, D. Das, D. Akhmetov, and C. Cordeiro, "Overview and Performance Evaluation of Wi-Fi 7," *IEEE Communications Standards Magazine*, vol. 6, no. 2, pp. 12–18, 2022.
- [8] S. Adhikari and S. Verma, "Analysis of Multilink in IEEE 802.11be," *IEEE Communications Standards Magazine*, vol. 6, no. 3, pp. 52–58, 2022.

- [9] K. Huang, L. Huang, Y. Quan, H. Du, C. Luo, L. Lu, and R. Hou, "Multi-link Channel Access Schemes for IEEE 802.11be Extremely High Throughput," *IEEE Communications Standards Magazine*, vol. 6, no. 3, pp. 46–51, 2022.
- [10] N. Korolev, I. Levitsky, and E. Khorov, "Analyses of NSTR Multi-link Operation in the Presence of Legacy Devices in an IEEE 802.11be Network," in *Proc. IEEE CSCN*, Dec. 2021.
- [11] N. Korolev, I. Levitsky, I. Startsev, B. Bellalta, and E. Khorov, "Study of Multi-link Channel Access without Simultaneous Transmit and Receive in IEEE 802.11be Networks," *IEEE Access*, vol. 10, pp. 126 339–126 351, 2022.
- [12] S. Naribole, S. Kandala, W. B. Lee, and A. Ranganath, "Simultaneous Multi-channel Downlink Operation in Next Generation WLANs," in *Proc. IEEE GLOBECOM*, Dec. 2020.
- [13] M. Carrascosa-Zamacois, L. Galati-Giordano, A. Jonsson, G. Geraci, and B. Bellalta, "Performance and Coexistence Evaluation of IEEE 802.11be Multi-link Operation," in *Proc. IEEE WCNC*, Mar. 2023.
- [14] T. Song and T. Kim, "Performance Analysis of Synchronous Multi-radio Multi-link MAC Protocols in IEEE 802.11be Extremely High Throughput WLANs," *Applied Sciences*, vol. 11, no. 1, p. 317, 2021.
- [15] N. Korolev, I. Levitsky, and E. Khorov, "Analytical Model of Multi-link Operation in Saturated Heterogeneous Wi-Fi 7 Networks," *IEEE Wireless Communications Letters*, vol. 11, no. 12, pp. 2546–2549, 2022.
- [16] S. Jung, S. Choi, H. Kim, Y. Yoon, and H.-k. Son, "Modeling the Coexistence Performance between Wi-Fi 7 and Legacy Wi-Fi," in *Proc. IEEE/IFIP NOMS, Doctoral Symposium*, May 2024.
- [17] G. Bianchi, "Performance Analysis of the IEEE 802.11 Distributed Coordination Function," *IEEE Journal on Selected Areas in Communications*, vol. 18, no. 3, pp. 535–547, 2000.
- [18] D. Magrin, S. Avallone, S. Roy, and M. Zorzi, "Performance Evaluation of 802.11ax OFDMA through Theoretical Analysis and Simulations," *IEEE Transactions on Wireless Communications*, 2023.
- [19] T. R. Henderson, M. Lacage, and G. F. Riley, "Network Simulations with the ns-3 Simulator," in *Proc. ACM SIGCOMM*, Aug. 2008.
- [20] T. M. Inc., "MATLAB version: 9.12.0 (R2022a)," Natick, Massachusetts, United States, 2022. [Online]. Available: <https://www.mathworks.com>
- [21] —, "Optimization Toolbox version: 9.3 (R2022a)," Natick, Massachusetts, United States, 2022. [Online]. Available: <https://www.mathworks.com>



Youngkeun Yoon received the B.E. and M.E. degrees in radio engineering from Chungbuk National University, Cheongju, South Korea in 1997, 1999, respectively. Since 2000, he has been worked in Electronics and Telecommunications Research Institute (ETRI). He has been involved in the research of simulation and evaluation for the radio resource management based on the multiple cellular system since 2003. He also was a visitor researcher in Center for Communication Systems Research (CCSR), University of Surrey, UK from 2003 to 2004. He has been involved in the analysis of the impacts for interference between existing system and new system. Currently, his research interests are in system performance and evaluations, radio propagation, and artificial intelligence based on radio communication system.

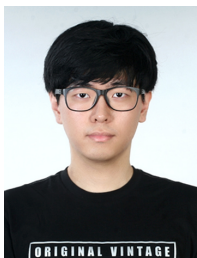


Ho-kyung Son received the B.S and M.S degrees in Electronic Engineering from Kyungpook National University, Daegu, Korea, in 1997 and 1999, and the Ph.D degree in the same university, Korea in 2013. From March 1999 to March 2000, she was a researcher of LG Information and Communication. Since May 2000, she has been with the Electronics and Telecommunications Research Institute (ETRI), Daejeon, Korea, where she is a principal researcher of radio resource research section of the Radio Research Division. Her research interests include

radio resource management, interference analysis between wireless communications, and radio propagation.



Suhwan Jung is a Ph.D. candidate at the Department of Electrical Engineering (EE), the Ulsan National Institute of Science and Technology (UNIST), Ulsan, Korea. He received his B.S. degree in the School of Electrical and Computer Engineering (ECE) from the UNIST in 2017, and his M.S. degree in the Department of Electrical Engineering (EE) from the UNIST in 2019. His research interest includes 5G/6G, V2X, and WLAN Multi-Link Operation (MLO).



Seokwoo Choi is a postdoctoral researcher at the School of Electrical Engineering, the Ulsan National Institute of Science and Technology (UNIST), Ulsan, Korea, since March 2025. He received his B.S. degree in Electrical and Computer Engineering from the UNIST, in 2017, and received Ph.D. degree in Electrical Engineering from UNIST, in 2025. His research interest includes 6G communications, WLAN, AI/ML, and low latency networking.



Hyoil Kim is a professor at the Department of Electrical Engineering, Ulsan National Institute of Science and Technology (UNIST), Korea. He received his B.S. degree in Electrical Engineering from Seoul National University in 1999, and M.S. and Ph.D. degrees in Electrical Engineering: Systems from the University of Michigan in 2005 and 2010, respectively. Before joining UNIST in 2011, he was a postdoctoral researcher in the IBM T.J. Watson Research Center, Hawthorne, NY, USA in 2010–2011. His research interest includes Hyperloop communications, B5G/6G, O-RAN, WLAN, AI/ML, V2X, UAM/satellite communications, and Dynamic Spectrum Access.